Original Study Open Access

Wojciech Pakos*, Andrzej Helowicz

Theoretical and numerical modeling of a shallow foundation stiffness based on the theory of elastic half-space

https://doi.org/10.2478/sgem-2024-0022 received May 3, 2024; accepted July 25, 2024.

Abstract: The paper presents the derivation of equations for the calculation of the spring constants k_{a} , k_{a} , and k_{b} and the spring coefficients β_{v} , β_{z} , and β_{ϕ} used in the modeling of a foundation with a rectangular base on elastic soil. All the equations were derived based on information provided in literature, for example, Barkan, Gorbunov-Possadov, and Whitman et al. To demonstrate the application of these equations in practice, two numerical models of a reinforced concrete frame structure that was built on soil were created using Abaqus FEA software. Model A represents a complex three-dimensional numerical model that consists of a reinforced concrete frame structure, which has a soil layer beneath it. Model B represents a simple three-dimensional numerical model consisting of a reinforced concrete frame structure, where the stiffness of the soil layer beneath the structure was modeled with vertical, horizontal, and rocking spring constants applied to the bottom of each foundation. Due to the nonlinear boundary condition used in the supports of the concrete frame model, such as contact and friction, all the involved loads were incorporated into a single load case, and a large displacement formulation was used in the analysis. The authors focused on the method of a simplified modeling of frame structures founded on soil. To conduct comparative analyses, two columns and two beams from each model were selected, from which the internal forces and displacements were compared. The findings of the comparative analysis are presented in tables and then discussed.

Keywords: design, frame structure, reinforced concrete, foundation stiffness, elastic subsoil

1 Introduction

A common practice when designing a building structure is to use simple types of supports, such as sliding, non-sliding, pinned or fixed supports, which do not reflect the actual interaction between the ground and the structure.

When designing a structure, the soil elasticity coefficient model is sometimes used, for example, the Winkler model [1]. This model assumes that the displacement w at a given point in the soil is directly proportional to the applied pressure p at that point, that is, p=Kw, where K is the modulus of the subgrade's reaction. In the Winkler model, the settlement of a given point only depends on the pressure applied at that point and does not depend on the pressures acting in the vicinity of that point. Adopting a simplified support model when designing a structure may lead to discrepancies between the work of the structure's numerical model and the real structure. Nevertheless, the Winkler model is still often used to analyze typical engineering structures, for example, foundation slabs and footings, piles, and railway tracks, as well as much more responsible and complex engineering structures. For example, in the paper [2], the Winkler model was used to calculate a hybrid retaining structure, and in the paper [3], it was used to analyze a caisson foundation subjected to static and dynamic loads.

In the following years, modifications of the Winkler model were developed. One of the example is a Pasternak's two-parameter model [4], which introduces an additional element on the surface of the Winkler model in the form of a shear working layer, ensuring the cooperation of the independent Winkler elastic bonds. In 1965, Kerr [5] proposed another two-parameter model consisting of two layers of elastic bonds connected by a shear transfer layer. Taylor and Chung in the paper [6] analyzed the contact stress distributions at the shallow foundation contact interface with an underlying real homogeneous, dry, compacted sand.

A more advanced approach, in comparison to the Winkler concept, to estimate the stiffnesses of a shallow

^{*}Corresponding author: Wojciech Pakos, Wroclaw University of Science and Technology, Faculty of Civil Engineering, pl. Grunwaldzki 11, 50-370 Wrocław, Poland, E-mail: wojciech.pakos@pwr.edu.pl, ORCID: https://orcid.org/0000-0002-3595-6577

Andrzej Helowicz, Wroclaw University of Science and Technology, Faculty of Civil Engineering, pl. Grunwaldzki 11, 50-370 Wrocław, Poland, ORCID: https://orcid.org/0000-0001-9527-1281



Table 1: Spring constants for a foundation with a rectangular base resting on elastic half-space [7], [8], [9].

Motion	Spring constant		Reference
Vertical	$K_z = \frac{G}{1 - \nu} \beta_z \sqrt{A}$	(1) V	Barkan (1962)
Horizontal	$K_x = 2G(1+\nu)\sqrt{A}\beta_x$	(2) H. K,	Barkan (1962)
Rocking	$K_{\phi} = \frac{G}{1 - \nu} \beta_{\phi} 8ab^2$	(3) M	Gorbunov-Possadov (1961)

where G – shear modulus of soil, v – Poisson's ratio of soil, A – foundation area (A=2a2b), 2a – length of the foundation (along the axis of rotation for the case of rocking), 2b – width of the foundation (in the plane of rotation for the case of rocking), V, H, M – vertical, horizontal, and rocking forces, β_z , β_z , β_ϕ – nondimensional coefficients of spring constants for a rectangular foundation, and K_x , K_x , K_y – vertical, horizontal, and rocking spring constants.

foundation model is based on the theory of elastic halfspace. The publications of researchers, such as Whitman and Richart [7], Lambe and Whitman [8], Richart, Woods and Hall [9], Braja M. Das et al. [10], and Fattah et al. [14], provide simple equations for determining the vertical, horizontal, and rocking spring constants that represent a linear relation between the applied loads and displacements of the foundation. This, in turn, implies a linear stress-strain relation for the soil (Fig. 1 and Tab. 1).

Based on the given equations for the spring constancies, the vertical (w), horizontal (u), and rocking (ϕ) displacements of a given foundation block with applied load can be calculated from the following equations: $w=V/K_z$, $u=H/K_y$, $\phi=M/K_\phi$.

Equations 2 and 3 in Table 1 were derived for a rigid foundation with a rectangular base. For the case of horizontal movement, the spring constant was derived by assuming a uniform distribution of shear stresses on the contact surface and by calculating the average horizontal displacement of this surface [11]. In works [7] to [10], it is stated that the spring constants K_x and K_z , which represent horizontal and vertical motion, respectively, were derived based on the assumptions given in the work by Barkan [11]. In turn, the spring constant K_{ϕ} , representing rocking motion, is based on the assumptions given in the works of Gorbunov-Possadov [12], [13]. The final form of the equations for determining the spring constants K_x , K_z and K_{ϕ} as well as the nomograms (Fig. 2) for determining the spring coefficients β_z , β_ϕ and β_x , are provided in works [7] to [10].

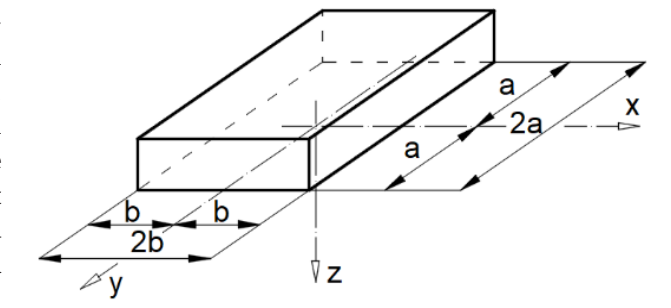


Figure 1: Scheme of a rectangular foundation.

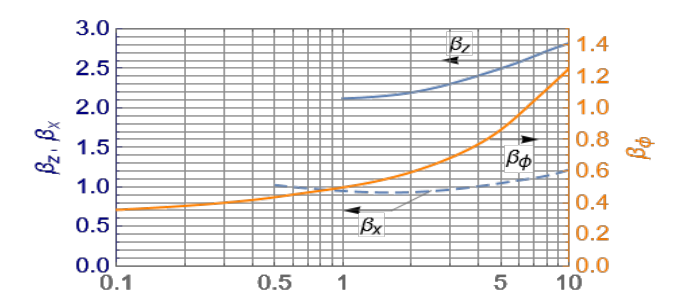


Figure 2: Coefficients β_{ν} , β_{ν} , and β_{μ} for a rectangular foundation base with regards to $\alpha = a/b$.

The above-mentioned works do not provide both the equations for determining the spring coefficients and the derivations of the equations for determining the spring constants. Therefore, based on the assumptions given by Barkan and Gorbunov-Possadov, the equations for the spring constants K_z , K_ϕ , and K_x and the spring coefficients β_z , β_ϕ , and β_x were derived in this paper. The values of elastic constants calculated on the basis of the derived equations were used in the numerical model of the concrete 3D frame (Fig. 6).

2 Determination of spring constants for a rigid foundation with a rectangular base resting on elastic half-space

2.1 Formula for spring constant K_z (vertical motion)

Barkan et al. [11] presented the results of many field tests that aimed to determine the compression-bearing capacity for different types of soil. The field tests consisted of load tests in which a concentrated load was transferred to the soil by a rigid bearing plate. Based on these findings, Barkan [11] stated that within a certain range, there is a proportional relationship between the elastic settlements of the foundation and the external uniform pressure acting on the soil, that is,

$$p_z = c_u S_e \tag{4}$$

where c_u is the coefficient of proportionality (called the coefficient of the elastic uniform compression of soil) and S_e is the elastic settlement of the bearing plate due to the external pressure p_z .

When assuming that the foundation consists of an absolutely flexible plate uniformly loaded by a vertical pressure, the stresses in the soil under the foundation are distributed uniformly, but settlement under the foundation varies. For an absolutely flexible foundation, the coefficient of elastic uniform compression is the ratio of uniform pressure to the average settlement value. Therefore, after transformation, equation (4) can be written in the following form:

$$p_z = c_u S_{av} \tag{5}$$

Furthermore, Barkan [11] assumed that

$$S_e = S_{\rm av} \tag{6}$$

and by using the work given by Schleicher [15], he gave the solution for an absolutely flexible foundation with a rectangular base. According to his solution, the average settlement value can be determined using the following equation:

$$S_{av} = \frac{1 - v^2}{E} \sqrt{A} \frac{1}{\pi \sqrt{\alpha}} \left[\ln \frac{\sqrt{1 + \alpha^2} + \alpha}{\sqrt{1 + \alpha^2} - \alpha} + \frac{1}{\sqrt{1 + \alpha^2} - 1} - \frac{2}{3} \frac{(1 + \alpha^2)^{\frac{3}{2}} - (1 + \alpha^3)}{\alpha} \right] p_z$$
(7)

where: $\alpha = a/b$, E – Young's modulus of soil, ν – Poisson's ratio, A – foundation area A=2a2b, and p_z – uniform pressure ($p_z=V/A$).

By dividing both sides of equation (7) by p_z and by performing its transformation, equation (7) can be written in the following form:

$$\frac{p_z}{S_{av}} = \frac{E}{1 - v^2} \frac{1}{\sqrt{A}} c_s \tag{8}$$

where

$$c_{s} = \frac{\pi\sqrt{\alpha}}{\ln\frac{\sqrt{1+\alpha^{2}}+\alpha}{\sqrt{1+\alpha^{2}}-\alpha} + \alpha\ln\frac{\sqrt{1+\alpha^{2}}+1}{\sqrt{1+\alpha^{2}}-1} - \frac{2}{3}\frac{(1+\alpha^{2})^{\frac{3}{2}}-(1+\alpha^{3})}{\alpha}}$$
(9)

Substituting $p_z = V/A$ and E = 2G(1+v) into equation (8) and making minor transformations of it, the following can be obtained:

$$K_z = \frac{V}{S_{\text{av}}} = \frac{G}{1 - \nu} \sqrt{A} \,\beta_z \tag{10}$$

where spring coefficient β_z can be written as

$$\beta_z = 2 c_s \tag{11}$$

2.2 Equation for spring constant K_{ϕ} (rocking motion)

The formulas given by Gorbunov-Possadov in papers [12] and [13] were used to derive the equation for spring constant K_{ϕ} . The adopted denotation of the foundation geometry and its axis layout for the rocking motion are shown in the Figure 3.



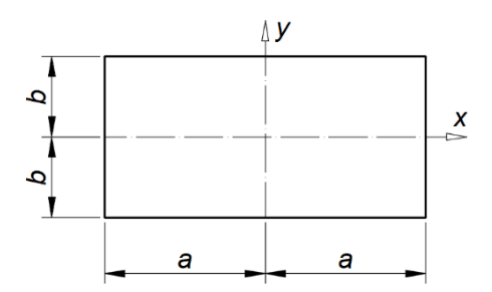


Figure 3: Scheme of a foundation with a rectangular base according to Gorbunova-Possadov [12], [13].

Gorbunova-Possadov, in his studies [12] and [13], gave formulas for determining the angles of rotation of a rigid rectangular foundation founded on soil and loaded by moments M_{ν} and M_{ν} :

$$tg\phi_{x} = \frac{1 - v^{2}}{F} K_{1} \frac{M_{x}}{a^{3}}$$
 (12)

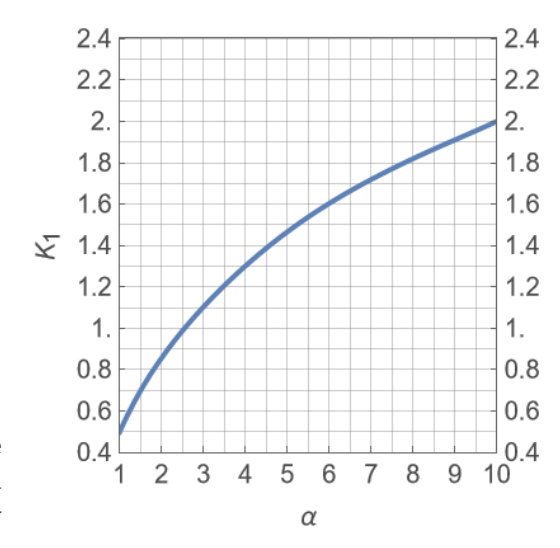
$$tg\phi_{y} = \frac{1 - v^{2}}{E} K_{2} \frac{M_{y}}{h^{3}}$$
 (13)

The coefficients K_1 and K_2 in these formulas are determined by using nondimensional reaction soil pressure equations, which are expressed by using power polynomials of the fifth and seventh degree or by using graphs (Figure 4a, b). The graphs show more accurate values of these coefficients than those calculated by the polynomials. Both the values of the coefficients calculated from the polynomials and those read from the graphs depend on the ratio of the dimensions of the foundation sides, that is, $\alpha = a/b$. Derived equations (14) and (15) describe the values variation of the coefficient K_1 and K_2 presented in Figure 4a and 4b.

$$K_1 = 2.6(1 - e^{(0.222\alpha^{0.81})})$$
 (14)

$$K_2 = 0.85 (1 - e^{(0.9\alpha^{-1})})$$
 (15)

The polynomial coefficients are determined by assuming that the foundation base adheres closely to the ground, that is, there is a compliance of vertical displacements of soil and the foundation base at each point. In addition, the friction between the soil and the base is omitted. Moment M_{ν} acts in a vertical plane parallel to the longer side of the rectangular base. Moment M_{ν} acts in a vertical plane parallel to the shorter side of the rectangular base [13].



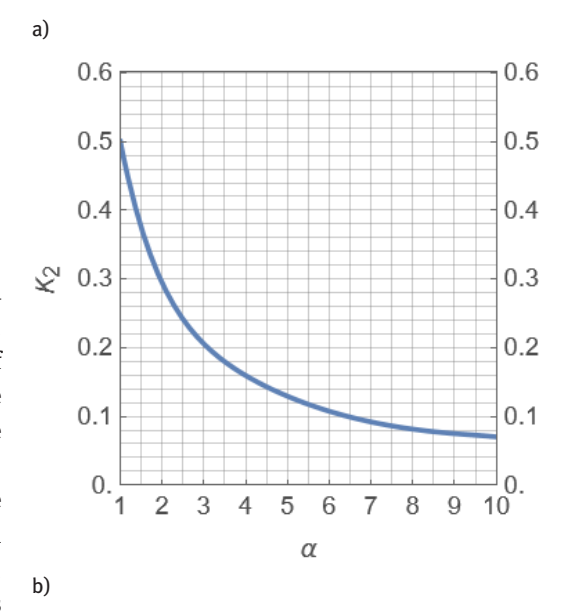


Figure 4: Graphs for determining the coefficients K_{a} (a) and K_{a} (b) used in equations (12) and (13). The graphs were prepared by the authors based on works [12] and [13].

2.2.1 Formula for spring constant K_{a}^{x} , that is, K_{a} from the action of moment M

By dividing equation (12) by moment M_{ν} and by making a simple transformation of this equation, the following can be obtained:

$$\frac{M_x}{\mathrm{tg}\phi_x} = \frac{E}{1 - v^2} \frac{a^3}{K_1} \tag{16}$$

By substituting $E=2G(1+\nu)$, one can get

$$\frac{M_x}{\mathrm{tg}\phi_x} = \frac{2G}{1-\nu} \frac{a^3}{K_1} \tag{17}$$

Knowing that A=2a2b, and $\alpha=a/b$, and thereby $a=1/2\sqrt{\alpha A}$, equation (17) can be written as

$$K_{\phi}^{x} = \frac{M_{x}}{\text{tg}\phi_{x}} = \frac{G}{1 - \nu} \frac{1}{K_{1}} \frac{1}{4} \alpha \, 8ba^{2}$$
 (18)

and finally as

$$K_{\phi}^{x} = \frac{G}{1 - \nu} \beta_{\phi}^{x} 8ba^{2} \tag{19}$$

where

$$\beta_{\phi}^{x} = \frac{1}{4} \frac{1}{K_1} \alpha \tag{20}$$

 $\beta_{\phi}^{\ x}$ is the spring coefficient and $K_{\phi}^{\ x}$ is the spring constant for a rectangular base in the direction of its greater rigidity.

2.2.2 Formula for spring constant $K_{\phi}^{\ y}$, that is, K_{ϕ} from the action of moment M_{ν}

By dividing equation (13) by moment M_y and by making a simple transformation of this equation, the following can be obtained:

$$\frac{M_y}{\text{tg}\phi_v} = \frac{E}{1 - v^2} \frac{b^3}{K_2}$$
 (21)

By substituting $E=2G(1+\nu)$, one can get

$$\frac{M_y}{\text{tg}\phi_y} = \frac{2G}{1 - v} \frac{b^3}{K_2}$$
 (22)

Given that A=2a2b, and $\alpha=a/b$, and thereby $b=1/2\sqrt{A/\alpha}$, equation (22) can be written as

$$K_{\phi}^{y} = \frac{M_{y}}{\text{tg}\phi_{y}} = \frac{G}{1 - v} \frac{1}{K_{2}} \frac{1}{4\alpha} 8ab^{2}$$
 (23)

and finally as

$$K_{\phi}^{y} = \frac{G}{1 - v} \beta_{\phi}^{y} 8ab^{2}$$
 (24)

where

$$\beta_{\phi}^{y} = \frac{1}{4} \frac{1}{K_{2}} \frac{1}{\alpha} \tag{25}$$

 β_{ϕ}^{y} is the spring coefficient and K_{ϕ}^{y} is the spring constant for a rectangular base in the direction of its lower rigidity.

For the purposes of this paper, and to standardize and conform to the description given in Figure 5, in the derivations of the equations for the spring constants K_x and K_z , the symbols in formulas (12) and (13) have been changed in the further part of this chapter. It was assumed that the rocking motion takes place along the X axis, and therefore, in accordance with works [7] to [9], 2b is the width of the foundation base (along the axis of rotation for rocking motion) and 2a is the length of the foundation base (in the plane of rotation for rocking motion).

Based on the adopted assumptions, the spring constant K_{ϕ} and the spring coefficient β_{ϕ} were derived for the oscillating motion. Their values are shown in Figure 2.

2.2.3 Spring constant K_{ϕ} for a rectangular base in the direction of lower stiffness, that is, $\alpha = a/b = (1 \div 0.1)$

Based on equation (26) and by making an additional transformation that is similar to those made in equations (21) to (25), the equation for the spring constant for a foundation in the direction of its lower stiffness can be obtained:

$$tg\phi_{\mathcal{V}} = \frac{1 - v^2}{F} \widetilde{K}_2 \frac{M}{a^3}$$
 (26)

$$K_{\phi} = \frac{G}{1-\nu} \beta_{\phi} 8ba^2 \tag{27}$$

where

$$\beta_{\phi} = \frac{1}{4} \frac{1}{\widetilde{K}_2} \alpha \tag{28}$$

 \widetilde{K}_2 is the coefficient for determining the angles of rotation of a rigid foundation with a rectangular base under the action of rocking moment M (read from the graph in Figure 4b). To calculate this coefficient, the range of values of $\alpha=a/b=(1\div10)$ should be replaced by $\alpha=a/b=(1\div0.1)$. The replacement of coefficient α (read from the graph in Figure 4b) is due to the fact that Gorbunov-Possadov considered that the foundation bends in two directions,





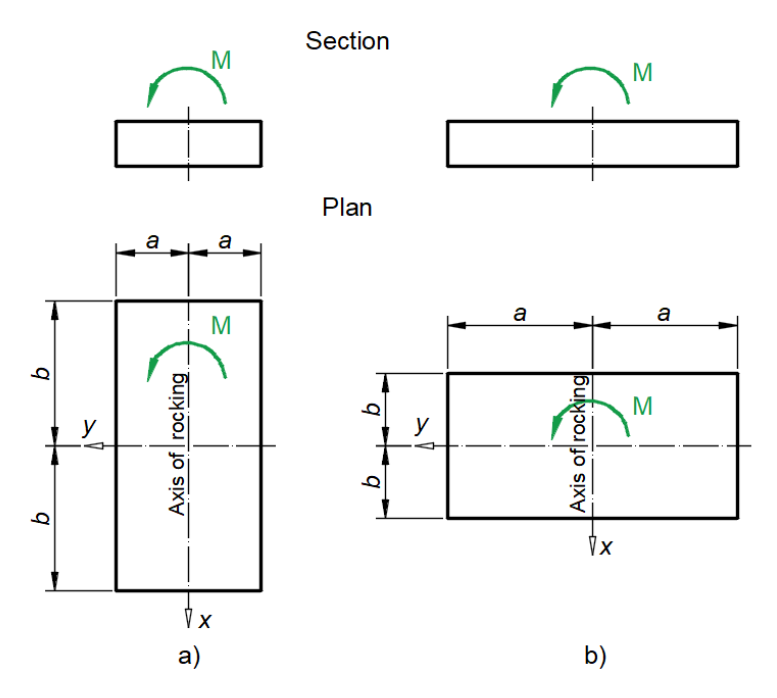


Figure 5: Notations for the equation for the spring constant in the case of rocking motion: (a) for $\alpha = a/b = (1 \div 0.1)$; (b) for $\alpha = a/b = (1 \div 10)$.

relative to the X and Y axes, with a ratio of the coefficient $\alpha = a/b = (1 \div 10)$. However, in the derivation of the spring constant equation K_{ϕ} , the authors assumed that the foundation only bends in one direction, relative to the X axis of rotation and with a ratio of a/b varying from 0.1 to 10, that is, for lower stiffness, it is $\alpha = a/b = (1 \div 0.1)$ and for higher stiffness, it is $\alpha = a/b = (1 \div 10)$.

2.2.4 Spring constant K_{ϕ} for a rectangular base in the direction of higher stiffness, that is, $\alpha = a/b = (1 \div 10)$

Based on equation (29), and by making an additional transformation similar to those made in equations (16) to (20), the equation for the spring constant for a foundation in the direction of its higher stiffness can be obtained:

$$tg\phi_{y} = \frac{1 - v^{2}}{E} K_{1} \frac{M}{a^{3}}$$
 (29)

$$K_{\phi} = \frac{G}{1 - \nu} \beta_{\phi} 8ba^2 \tag{30}$$

where

$$\beta_{\phi} = \frac{1}{4} \frac{1}{K_1} \alpha \tag{31}$$

 K_1 is the coefficient for determining the angles of rotation of a rigid foundation with a rectangular base under the action of rocking moment *M* (read from the graph in Figure 4a).

2.3 Equation for spring constant K_{\downarrow} (horizontal motion)

Based on the assumptions given by Barkan [11], the equations for spring constant K_{ν} and coefficient β_{ν} were derived, with a theoretical basis being used to derive these equations.

If the foundation is subjected to a horizontal force applied at the level of the contact surface of the foundation base and the soil, the foundation will move in the direction of this force (Table 1).

From the experimental data given by Barkan [11], under conditions similar to steady-state conditions for soil under compression, it can be concluded that there is a linear relationship between the base sliding motion and the average shearing stress developed along the base contact surface with the soil, that is,

$$\tau_{\rm av} = c_{\tau} S_e' \tag{32}$$

where au_{av} is the average shearing stress in the soil at the plane of contact with the foundation and S_e' is the elastic part of the total horizontal sliding of the foundation base under the action of τ_{av} . Barkan [11] assumed that the elastic part of the total horizontal sliding is equal to the average value of the horizontal sliding $S'_e = S'_{av}$ along the surface area A=2a2b, and he gave the following equation:



$$S'_{av} = \frac{4\alpha}{\pi} \frac{1 - v^2}{E} \left(\frac{1}{\alpha} \sinh^{-1}\alpha + \sinh^{-1}\frac{1}{\alpha} - \frac{1}{3} \left[\frac{1}{\alpha^2} \left(\sqrt{1 + \alpha^2} - 1 \right) + \sqrt{1 + \alpha^2} - \alpha \right] + \frac{v}{1 + v} \left\{ \frac{1}{\alpha} \sinh^{-1}\alpha + \frac{1}{3} \left[\sqrt{1 + \alpha^2} - \alpha - \frac{2}{\alpha^2} \left(\sqrt{1 + \alpha^2} - 1 \right) \right] \right\} \right) \tau_{av}$$
(33)

where $\alpha = a/b$, E is the Young's modulus of soil, and v is the Poisson's ratio.

Knowing that A=2a2b, and by substituting $\tau_{av}=H/A$ and $\alpha = 1/2\sqrt{A} \alpha$ into equation (33), and by making simple transformations, the following can obtained:

$$\frac{H}{S_{\rm av}'} = \frac{E}{1 - v^2} \sqrt{A} k_{\tau} \tag{34}$$

where

$$k_{\tau} = \frac{\pi}{2\sqrt{\alpha} \left(\frac{1}{\alpha} \sinh^{-1}\alpha + \sinh^{-1}\frac{1}{\alpha} - \frac{1}{3} \left[\frac{1}{\alpha^{2}} (\sqrt{1 + \alpha^{2}} - 1) + \sqrt{1 + \alpha^{2}} - \alpha \right] + \frac{\nu}{1 + \nu} \left\{ \frac{1}{\alpha} \sinh^{-1}\alpha + \frac{1}{3} \left[\sqrt{1 + \alpha^{2}} - \alpha - \frac{2}{\alpha^{2}} (\sqrt{1 + \alpha^{2}} - 1) \right] \right\}} \right)$$
(35)

By substituting $E=2G(1+\nu)$ into equation (32), K can be derived:

$$K_x = \frac{H}{S'_{av}} = 2G(1+\nu)\sqrt{A}\,\beta_x$$
 (36)

where

$$\beta_x = \frac{k_\tau}{1 - \nu^2} \tag{37}$$

It should be noted that in papers [7] to [9], the values of the spring coefficient β_{ν} were determined by assuming that the Poisson's ratio of the soil has a constant value v = 0.3. From equation (35) derived by the authors, spring coefficient β_{ν} can be additionally calculated for various values of the Poisson's ratio.

3 Description of the model

It is often impractical to model an entire structure with complex three-dimensional solid elements. A very complex numerical model can lead to more inaccurate results than those predicted by simpler models, such as grillage or 3D frame. Due to the complex nonlinear nature of soil behavior under loads, the analysis was limited to the simple assumption that the mechanical parameters of soil strictly follow Hooke's law. Furthermore, it was assumed that the pressure in the soil under the footing foundation is lower than the soil's bearing capacity. This is usually the case with a typical foundation design. For the purpose of the analysis, complex and simple models of the concrete 3D frame structure (Fig. 6) were built using Abagus FEA software [16].

Complex model A (Fig. 7) consists of the concrete 3D frame structure and the soil layer beneath it.

In this model, the interlayer interaction between the bottom surface of the footing foundation (the base) and the top surface of the soil layer was modeled as a standard contact surface-to-surface type discretization method with a finite sliding formulation. Furthermore, normal behavior with "hard" contact pressure overclosure and allowable separation after contact was applied. The adopted contact method permits some relative motion of the contact surfaces. Contact interaction properties are a tangential behavior with a static coefficient of friction μ equal to 0.58. This coefficient was calculated based on the assumption that the internal angle of friction between the concrete and the soil material is the same as the internal angle of friction of the soil layer beneath the footing foundation. In turn, simple model B (Fig. 8) only consists of the concrete 3D frame structure.

The missing soil layer in this model was replaced by spring constants derived for a rigid rectangular foundation resting on an elastic half-space. Five spring constants were applied to the center of the bottom surface of each footing foundation. Three of them were responsible for vertical and horizontal motion, and the remaining two were responsible for rocking motion around the X and Y axes. Model B represents an engineering approach to the design of a 3D frame structure resting on soil. In model A, it was assumed that the soil layer beneath the structure has a constant and uniform depth of 20.0 m below the footing foundations (Figure 7). In all the numerical models, the frame structure is represented by 264 Euler-Bernoulli two-node cubic beam elements of type B33. Each column consists of 16 beam elements: beam B1 consists of 48 beam elements and beam B2 consists of 24 beam elements. All the beams are connected together, so that there is no relative motion between them. Kinematic type couplings were used to connect the beam elements with the solid elements that represent the footing foundation. In this connection, the bottom node of the beam element is the control point and the upper surface of the footing foundation directly under the column is the constraint region. These connections are shown in Figure 8. The footing foundations are represented by 10,200 general purpose eight-node linear hexahedral elements of type C3D8 that have hourglass element controls. Each corner footing foundation consists of 1350 elements, while



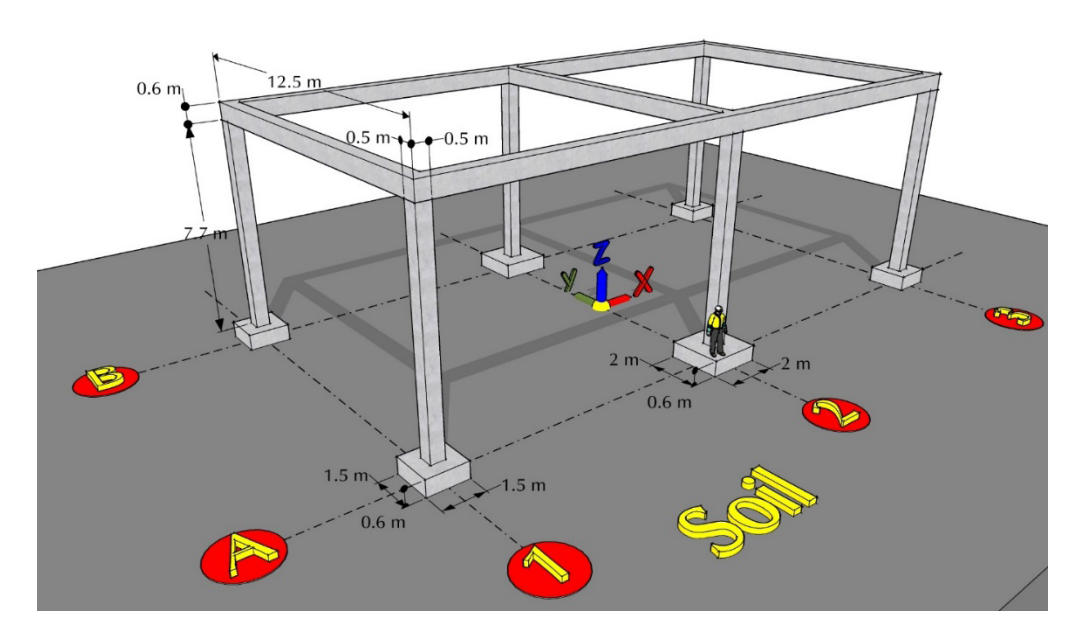


Figure 6: The analyzed 3D frame.

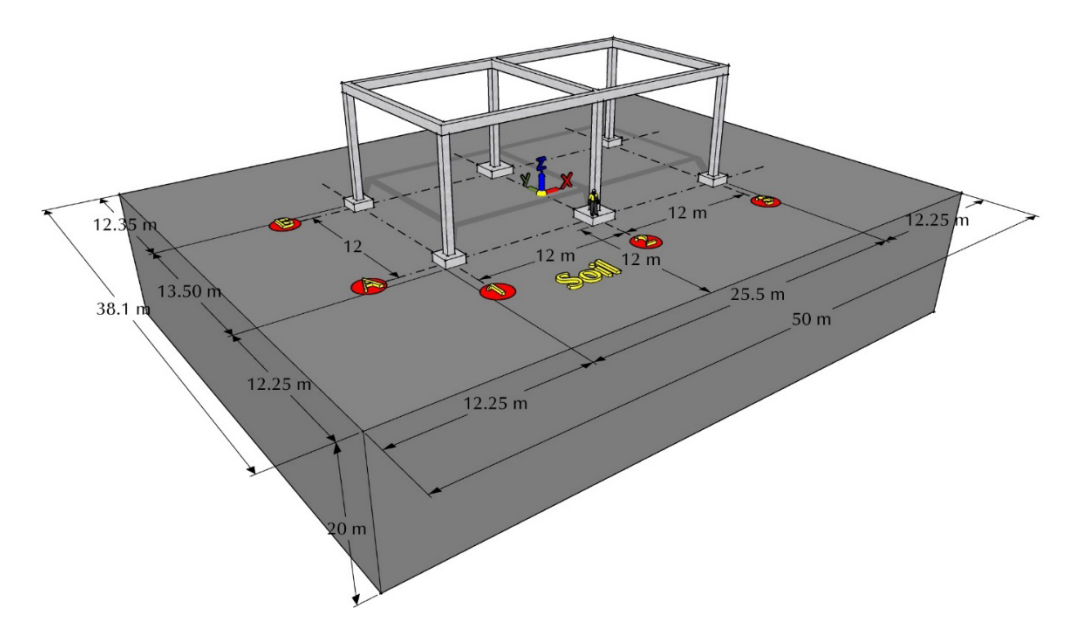


Figure 7: Axonometric view of complex model A.

each inner footing foundation consists of 2400 elements. The same element type was used to build the block of the soil layer beneath the footing foundation (Figure 9).

The total number of elements representing the soil layer beneath the footing foundation is equal to 476,160. Material constants, such as the internal angle of friction (ϕ) , Young's modulus (E), and the Poisson's ratio (v) of the materials selected for the analysis, are presented in Table 2. The soil angle of friction was used to assess the coefficient of friction between soil and the concrete surface, which was used to model the contact interaction in model A.

In Table 2, the following designations were used: E – modulus of elasticity, ν – Poisson's ratio, ϕ – soil internal angle of friction, G – soil shear modulus, L – length of the foundation (in the plane of rotation for the case of rocking), B – width of the foundation (along the axis of rotation for the case of rocking).

The dimensions of the footing foundation and the soil layer beneath the footing are shown in Figures 6 and 7. Each vertical surface of the soil layer only has a horizontal restraint applied perpendicularly to each surface. The bottom surface of this layer only has a vertical restraint applied perpendicularly to this surface. In addition, it

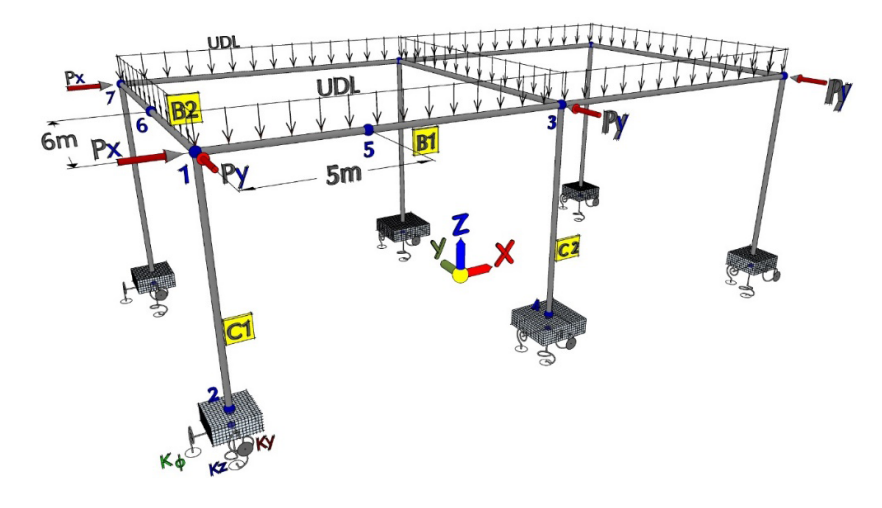


Figure 8: Axonometric view of simple model B.

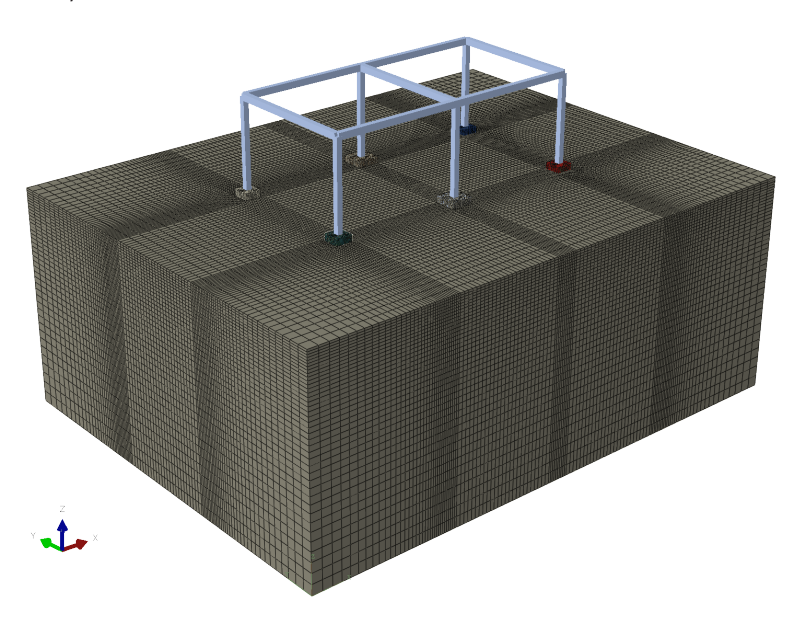


Figure 9: Finite element mesh of complex model A.

Table 2: Material properties used in the analysis.

Model	А, В
Soil	Loose sand [17]
E_s [MN/m ²]	40 (Middle range value)
ν	0.3
ϕ	30 (Model A)
G [MN/m ²]	15.385
$L \times B$ [m]	1.5 × 1.5
$L \times B$ [m]	2.0 × 2.0
Frame structure	Concrete C50/60
E_{cm} [MN/m ²]	37,000
V	0.2

was assumed that the foundations are not backfilled. This situation may occur during temporary works in the vicinity of the foundation.

In Table 3, the following designations were used: (β_{s}) β_{z} , β_{z}) – spring coefficients, (K_{z}, K_{z}, K_{z}) – spring constants.

The nominal loads applied to the structure are shown in Figure 8 and Table 4.

In model A, the superposition principle cannot be used in the calculations of this structure due to the nonlinear boundary condition used in the frame model supports, such as contact and friction. For this reason, in both models, all the loads involved were incorporated into a single load case, and the large displacement formulation was used in the static analysis. The self-weight of the soil layer in model A was omitted in the analysis.



Table 3: Calculated spring constants used in model B.

In the corner footing	In the inner footing	Units
$\boldsymbol{\beta}_{x} = \boldsymbol{\beta}_{y}$	_= 0.956	
β_z =	2.113	
$oldsymbol{eta}_{\phi X} = oldsymbol{\mu}$	$B_{\phi Y} = 0.49$	
$k_x = k_y = 57,374$	$k_x = k_y = 76,498$	[kN/m]
$k_z = 69,668$	$k_z = 92,891$	
$k_{\phi X} = k_{\phi Y} = 36,381$	$k_{\phi X} = k_{\phi Y} = 86,235$	[kN/m/rad]

Table 4: Load applied to the structure.

Load type	Value
Self-weight of the concrete frame structure (SW)	24 kN/m³
Uniform distributed load (UDL)	20 kN/m
Concentrated force Px and Py	10 kN

4 Comparative analysis

The subjects of the analysis were the two columns C1 and C2 and the two beams B1 and B2 shown in Figure 6. In each of these structural elements, the values and distribution of the internal forces and displacements obtained from spatial frame models A and B were compared and analyzed. The values of the linear displacements, internal forces, and bending moments were consistent with the global axes coordinate system shown in Figure 6. The calculation results for the columns and beams are shown in Tables 5-7.

4.1 Columns C1 and C2

Tables 5 and 6 show the values of the displacements, internal forces, and bending moments at the top and bottom of the C1 and C2 columns of the analyzed models of concrete 3D frames A and B.

The relative error presented in the tables is calculated according to the following equation:

$$Error = \frac{value \ model \ B - value \ model \ A}{value \ model \ A} \ [\%]$$

In Tables 5 and 6, the following designations were used: U_y , U_y , U_z are linear displacements, N is the axial force, T_{v} and T_{x} are shear forces, and M_{v} and M_{v} are bending moments.

From the calculation results for columns C1 and C2 in frames A and B, the following can be concluded:

- 1. The values of displacements U_x , U_z , and U_z in column C1 in both frames A and B, as well as in column C2 in both frames A and B in all analyzed nodes, are very similar. However, the columns in the simple frame model B have slightly larger displacements than the columns in complex model A by about 0.2 mm in the horizontal direction and about 0.9 mm in the vertical direction in all the analyzed nodes.
- The values of the axial forces, shear forces, and bending moments in column C1 in both frames A and B, as well as in column C2 in both frames A and B in all the analyzed nodes, are very similar. The difference in values in all the analyzed nodes does not exceed 0.6 kN in the case of all the forces, and it does not exceed 2.7 kNm in the case of all the bending moments.

4.2 Beams B1 and B2

Tables 7 and 8 show the values of the displacements, internal forces, and bending moments in beams B1 and B2 in the analyzed models of concrete 3D frames A and B.

From the calculation results for beams B1 and B2 in frames A and B, the following can be concluded:

- The values of displacements U_{\cdot} , U_{\cdot} , and U_{\cdot} in beam B1 in both frames A and B, as well as in beam B2 in both frames A and B in all the analyzed nodes, are very similar. However, the beams in simple frame model B have slightly larger displacements than the beams in complex model A by about 0.2 mm in the horizontal direction and by about 0.9 mm in the vertical direction in all the analyzed nodes.
- The values of the axial forces, shear forces, and bending moments in beam B1 in both frames A and B, as well as in beam B2 in both frames A and B in all the analyzed nodes, are very similar. The difference in the values in all the analyzed nodes does not exceed 0.6 kN in the case of all the forces and does not exceed 1.8 kNm in the case of all the bending moments.

5 Conclusions

Based on the results obtained from the analyzed example of a 3D frame, it can be concluded that the derived equations for spring constants, which describe the impact of a foundation placed on the ground, can be used in the design of frame structures. This information is particularly

Table 5: Results for columns C1.

	Column	C1				
	Node 1	1	1	Node 2		
	Model A	Model B	Error	Model A	Model B	Error
Ux [mm]	2.2	2.3	4.5%	-0.4	-0.5	25.0%
Uy [mm]	3.5	3.7	5.7%	-0.6	-0.6	0.0%
Uz [mm]	-5.0	-5.7	14.0%	-4.7	-5.4	14.9%
N[kN]	-299.2	-298.9	-0.1%	-344.2	-343.9	-0.1%
Ty [kN]	-21.1	-20.6	-2.4%	-21.1	-20.6	-2.4%
Tx [kN]	-16.6	-16.1	-3.0%	-16.6	-16.1	-3.0%
Mx [kN m]	161.0	159.1	-1.2%	-7.9	-5.3	-32.9%
My [kN m]	-124.3	-123.0	-1.0%	8.4	5.6	-33.3%

Table 6: Results for columns C2.

	Column	C2				
	Node 3			Node 4		
	Model	Model	Error	Model	Model	Error
	Α	В		Α	В	
U_x [mm]	2.1	2.2	4.8%	0.2	0.2	0.0%
U_{y} [mm]	3.2	3.3	3.1%	-0.4	-0.5	25.0%
U_z [mm]	-6.5	-7.3	12.3%	-6.0	-6.9	15.0%
N [kN]	-532.2	-532.2	0.0%	-577.2	-577.2	0.0%
$T_{y}[kN]$	-23.6	-23.1	-2.1%	-23.6	-23.1	-2.1%
$T_{x}[kN]$	4.5	4.6	2.2%	4.5	4.6	2.2%
M_{x} [kNm]	167.0	165.3	-1.0%	-21.5	-19.2	-10.7%
M_y [kNm]	21.5	22.2	3.3%	-14.7	-14.5	-1.4%

Table 7: Results for beam B1.

important when designing a structure founded on the ground. The use of simple types of supports in the numerical model, such as sliding, nonsliding, pinned, or fixed supports, which do not reflect the actual interaction of the structure with the ground on which it will be founded, leads to the incorrect design of the structure. As a result, the calculated values of displacements and internal forces in the designed structure will not correspond to the values of displacements in the actual structure. Consequently, some elements of the designed structure will be incorrectly over-reinforced and others will be incorrectly under-reinforced. Cracks may appear on the surfaces of the under-reinforced structural elements and, in some cases, the structural elements may break and cause the entire structure to collapse. The following additional conclusions can be drawn from the presented comparative analysis of the two 3D concrete frame models, which differ significantly in terms of the complexity of the construction of their numerical models:

- The equations derived for the calculation of the spring coefficients and constants can be used to simplify the numerical model of a structure founded on soil.
- The results of the comparative analysis of four structural elements of two 3D frames show that there is a good consistency between the results obtained from complex model A and simple model B. Of the four elements selected for the comparative analysis, including two columns and two beams from each 3D frame, the calculated displacements, internal forces, and moments are very similar in both frame models. The largest difference in the displacements and internal forces in all directions of the structural elements of both frames is equal to 0.9 mm and 0.6 kN, respectively. The largest difference in bending

	Node 1			Node 5	Node 5			Node 3			
	Model A	Model B	Error	Model A	Model B	Error	Model A	Model B	Error		
U_x [mm]	2.2	2.3	4.5%	2.10	2.20	4.8%	2.1	2.2	4.8%		
U_{y} [mm]	3.5	3.7	5.7%	3.40	3.50	2.9%	3.2	3.3	3.1%		
U_z [mm]	-5.0	-5.7	14.0%	-13.00	-13.90	6.9%	-6.5	-7.3	12.3%		
N [kN]	-26.3	-25.7	-2.3%	-26.30	-25.70	-2.3%	-26.3	-25.7	-2.3%		
$T_{y}[kN]$	131.7	131.6	-0.1%	2.50	2.40	-4.0%	-181.1	-181.2	0.1%		
$T_x[kN]$	-0.4	-0.4	0.0%	-0.40	-0.40	0.0%	-0.4	-0.4	0.0%		
M_{x} [kNm]	123.8	122.4	-1.1%	-228.60	-229.40	0.3%	409.7	409.3	-0.1%		
M_{y} [kNm]	-1.8	-2.0	11.1%	-0.10	-0.10	0.0%	2.4	2.6	8.3%		



Table 8: Results for beam B2.

	Node 1			Node 6	Node 6			Node 7		
	Model A	Model B	Error	Model A	Model B	Error	Model A	Model B	Error	
U_{x} [mm]	2.2	2.3	4.5%	2.2	2.3	4.5%	2.2	2.3	4.5%	
U_{y} [mm]	3.5	3.7	5.7%	3.5	3.7	5.7%	3.5	3.6	2.9%	
U_z [mm]	-5.0	-5.7	14.0%	-17.0	-17.8	4.7%	-5.1	-5.8	13.7%	
N [kN]	-30.8	-30.2	-1.9%	-30.8	-30.2	-1.9%	-30.8	-30.2	-1.9%	
$T_{y}[kN]$	152.4	152.3	-0.1%	-4.0	-4.1	2.5%	-160.4	-160.5	0.1%	
$T_{x}[kN]$	0.3	0.3	0.0%	0.3	0.3	0.0%	0.3	0.3	0.0%	
M _x [kNm]	-161.5	-159.7	-1.1%	304.0	305.1	0.4%	-209.7	-209.2	-0.2%	
M, [kNm]	1.6	2.0	25.0%	0.0	0.0	0.0%	-1.7	-2.0	17.6%	

- moments M_v and M_z does not exceed 2.7 kNm in the columns, and 1.8 kNm in the beams.
- Simplification of the numerical model of the design structure significantly reduces the time needed to build the model and perform its calculations. It also reduces the size of the output database files. The calculation time of the complex model A and the simple model B was 2560 and 18 sec, respectively. In addition, the output database file of complex model A contains 749.3 MB of data, while model B contains only 6.01 MB of data. It should be added that model A can be more optimized, which can speed up its calculation. The article presents a simple model of a structure with a simple load, while in practice, we encounter more complex models of structures. The simplified modeling method proposed by the authors will be much more beneficial due to its simplicity and much shorter calculation time.
- The derived equations for the spring constants can be used in engineering structure analysis software that is less numerically advanced than Abaqus FEA software.
- To correctly model a structure built on soil, it is imperative to correctly determine the elastic properties of the soil. On the basis of such data, a designer can develop a model of the structure founded on a specific soil. Therefore, close cooperation is required between a geotechnical engineer and a structural engineer when designing 3D frame structures built on soil.

Acknowledgements

The calculations were carried out using resources provided by Wroclaw Center for Networking and Supercomputing (https://wcss.pl), grant No. 554.

References

- [1] Winkler, E. (1867). Die Lehre von der Elastizitat und Festigkeit. Dominicus, Prague.
- Brząkała W., Herbut A. (2018). Application of the Winkler model to the calculation of a hybrid retaining construction. Acta Sci. Pol. Architectura, 17 (2), 37-51 (in Polish).
- Nikos Gerolymos, George Gazetas. (2006). Development of Winkler model for static and dynamic response of caisson foundations with soil and interface nonlinearities. Soil Dynamics and Earthquake Engineering, (26), 363–376.
- Pasternak, P. (1954). On a new method for analysis of foundations on an elastic base using two base parameters. Gosudarstvennoe Izdatelstro Liberaturi po Stroitelstvui Arkhitekture. Moscow (in Russian).
- Kerr, A. (1965). A study of a new foundation model. Acta [5] Mechanica, 135-147 (1965).
- Taylor, A.G.; Chung, J.H. (2022). Explanation and Application of the Evolving Contact Traction Fields in Shallow Foundation Systems. *Geotechnics*, (2), 91-113. https://doi.org/10.3390/ geotechnics2010004
- Whitman, R. V., and Richart, F. E., Jr. (1967). Design Procedures [7] for Dynamically Loaded Foundations. Journal of the Soil Mechanics and Foundations Division, 93(6), 169-193.
- Lambe, T. W., Whitman, R. V. (1969). Soil Mechanics, Wiley, New
- Richart, F. E., Woods, R. D., Hall, J. R., (1970). Vibrations of Soils and Foundations, Prentice-Hall.
- [10] Braja M. Das, Ramana, G. V. (2011). Principles of Soil Dynamics, Second Edition, Nelson Education.
- [11] Barkan, D. D. (1962). Dynamics of bases and foundations. New York: McGraw-Hill, (Translated from Russian).
- [12] Gorbunov-Possadov, M. I., Serebrajanyi, R. V. (1961). Design of Structures upon Elastic Foundations, Proc. 5th International Conference on Soil Mechanics and Foundation Engineering, (1), 643-648.
- [13] Gorbunov-Posadov, M. I. (1956). Obliczanie konstrukcji na podłożu sprężystym. Budownictwo i Architektura, Warszawa, (Translated from Russian).
- [14] Fattah, M. Y., Al-Azal Al-Mufty, A. A., Al-Badri, H. T. (2007). Design charts for machine foundations. Journal of Engineering, 4(13), 1940-1961. doi:10.31026/j.eng.2007.04.07.

- [15] Schleicher, F. (1926). Zur Theorie der Baugrundes. *Der Bauingenieur*, (48), 931-935.
- [16] Abaqus FEA software, Dassault Systemes, https://academy.3ds.com
- [17] Bowles, J. E. (1997). *Foundation analysis and design*. Fifth Edition. The McGraw-Hill Companies, Inc.